PROPELLER INDUCED GROUND VORTEX

Y. Yang, D.Ragni,
L. Veldhuis, G. Eitelberg
Y.Yang-1@tudelft

Keywords: *ground-vortex, propeller propulsion, vorticity, actuator disk, PIV*

Abstract

A study of the interaction of propeller generated thrust and the resulting flow field when the propeller is close to a solid surface is performed. The study involves both experiments in a wind tunnel with a real propeller as well as numerical evaluations where the propeller is modeled as an actuator disk. The interaction creates a ground vortex under certain conditions of thrust setting and ground proximity. In the present study the vortex is generated purely as a local phenomenon resulting from the propulsive action of the propeller and the presence of a solid surface in the area of interaction – no upstream source of vorticity in the form of a boundary layer or otherwise is required.

The actuator disk used is modified in order to account for the aerodynamic characteristics of standard profile designs resulting in the suction side of the disk generating the propulsive force and resulting in a stronger stream tube contraction on the upstream side of the propeller plane than on the downstream side. It is found that the resulting stream tube model can be effectively used to predict the trend of the numerically calculated occurrence of the ground vortex. For quantitative determination of the domain separation of vortex/no vortex an empirical coefficient has to be included in the presented simple model.

The experimental results, confirm the validity of the chosen approach. Due to the nature of the curved vortices in the flow, the unsteadiness of the flow could only be suppressed in the modeling, but not in the experiments.

1 Introduction

The ground- or fuselage vortex is a well-studied phenomenon in the context of avoiding damage to the aircraft propulsion during the engine run-up or taxiing. Notwithstanding the vast amount of studies concerning the suction tube analogy of an engine intake with continuous suction (e.g. De Siervi *et al*. [1]), there is little information about the direct effect of the vortex on the engine rotor, which could be either a fan or a propeller. It is in fact expected that the presence of a vortex at the entrance of an engine is affecting the loading of the rotor blades, having structural consequences even without foreign object damage. At the very least, in the experiments on that subject an extra excitation of vibrations of the rotating system has to be considered. The ground- or fuselage vortex can also contribute to the production of noise through adding an extra pressure fluctuation into the rotor flow field. Understanding the mechanism behind these detrimental effects and providing some guidance on to how to avoid them has been the driving motivation for the present study.

In view of the fuel saving potential of un-shrouded aircraft engines, a simple propeller was considered an appropriate object for studying the ground vortex phenomenon as it interacts with a rotor. The first question arising when addressing the above concerns is that of the unequivocal existence of the domains of occurrence of the ground vortex. Murphy [2] discusses the different literature sources providing domain separation in terms of the

suction tube height above ground and the ratio of the free-stream velocity to the intake velocity. In this model a linear relationship defines the separation line between the two domains, one where the ground vortex occurs and the other one where it does not. Murphy also shows the rather large scatter of the published data when it is organized in such a way. In a later publication, Murphy and MacManus [2] further discuss the ground vortex under headwind (and quiescent) conditions. In this paper the boundary layer thickness in headwind conditions is discussed in the context of the occurrence of the ground vortex phenomenon, although this does not provide a convincing description of the mechanism of the origin of the vortex in quiescent conditions with no boundary layer carrying vorticity. A discussion of the vortex generation with no recourse to the upstream boundary layer will follow below.

2 Mechanism of formation of the ground vortex

The generation and transport of vorticity is dealt with in many treatises and textbooks. One of the fundamental references is a summary by M. J. Lighthill [4], where the term vorticity flux from a solid wall $\vec{n}\cdot\sigma$ is introduced. This vorticity flux is the mechanism for transporting vorticity from the wall, where it is produced, into the flow field. In literature, considering the inlet vortex formation, it is usually discussed in the context of the vortex transport equation:

$$\frac{D\omega}{Dt} = \omega \cdot \nabla \mathrm{u} + \upsilon \nabla^2 \omega \qquad (2)$$

Since this equation does not contain any vorticity sources, a number of authors (e.g. De Siervi *et al.* [1], etc.) postulate and discuss different pre-existing concentrated vorticity regions which, when encountering local acceleration in the flow field, lead to vortex stretching and thereby to the formation of pronounced intake vortices as a result of pre-existing concentrated vortices, see Figure 1 from Murphy [2].

However, especially for the case of benign conditions where the wall boundary layer is thick, such as is the case when $u_\infty << u_i$, where u_i and u_∞ are the intake and free stream velocities respectively in the suction tube approximation, that there is no concentrated vorticity in the thick boundary layer. In fact, the vorticity which is initially concentrated on the solid boundary will diffuse into the flow and spread in a continuous manner across the whole boundary layer.

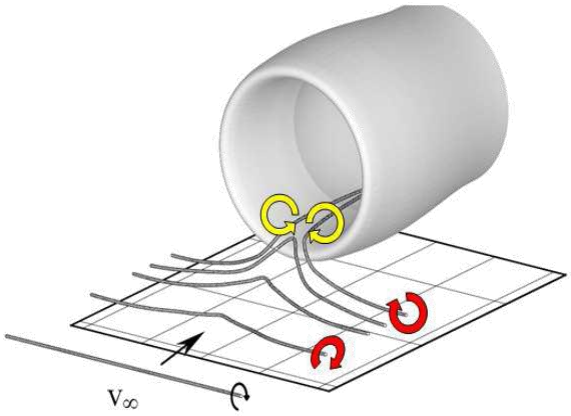

Figure 1 (from Murphy [2]): vortex stretching mechanism

In the previously quoted work by Murphy and MacManus([2],[3]), where the results from an extensive measurement program are summarized along with the ones from further literature, the discussion of domain is defined with the help of two non-dimensional parameters, the intake velocity u_i normalized with the free stream velocity u_∞ (u_i/u_∞), and the height of the inlet above ground h normalized with the diameter of the intake D, (h/D):

$$u_i/u_\infty = 8.5 \cdot h/D + 1.2 \qquad (1)$$

At intake velocity ratios above the straight line thus defined, a ground vortex should be present. In the case of the quiescent flow (u_∞=0), this relationship will always predict a ground vortex. Within the domain defined by the equation (1), above the line thus defined, another region, with the maximum of the strength of the ground vortex was also identified.

In the present paper it is proposed that the pressure drop against the ambient pressure, generated by the rotor plane in its propulsive

action, together with the free-stream dynamic pressure are the relevant parameters for the domain delineation. It is also proposed that the free-stream which needs to be considered is that of the relative motion between the aircraft and the stationary frame of reference, i.e. the runway is also moving with the velocity of the free-stream for the headwind condition and that the far-field boundary layer is not a dominant characteristic in this context.

Wu and Wu ([5], [6]) have considered the interactions between a solid surface and a viscous compressible flow field. The diffusion of wall parallel vorticity into the fluid (vortex line ascending pattern) as a result of wall parallel pressure gradients as well as the turning of the vorticity vector to produce a wall-normal component in three dimensional flows (the upturning mechanism) are discussed by those authors. This upturning is the result of the rotation of the wall shear stress vector τ field given by the above authors as:

$$\vec{n} \cdot \sigma = -\vec{n} \cdot (\nabla \times \vec{\tau}) \qquad (3)$$

where $\vec{n}$ indicates the wall normal unit vector. The upturning mechanism does not require a continuous line of vorticity to exist in the upstream flow field, and thus no Ω-shaped vortex is required to enter the rotor plane.

Fric and Roshko [7] provided a somewhat simplified description of the vortex generation mechanism for the case of a circular wall jet under conditions where the flow was incompressible and the walls were not accelerated. In their analysis the wall parallel vorticity production by the pressure gradient on the wall is considered as well as the gradients of the wall shear stress terms producing a wall normal component of vorticity. The generation of a wall-normal vorticity component requires a separation streamline to exist. The inverse is also valid; when there is a concentrated pressure field with a suction center on the wall causing separation, a wall-normal vorticity component is always produced.

Those two mechanisms, the pressure gradient and the wall shear stress gradients leading to separation, can produce enough vorticity to explain the existence and growth of the ground vortex. Since the vorticity created in the free-stream is not an a priory requirement for numerically reproducing the phenomenon, realistic boundary conditions on the ground plane representing the pressure distribution along the wall and the location of the separated streamline have to be generated. The boundary conditions on the solid surface (ground) are produced by utilizing an actuator disk model, modified for our purposes, immersed into the flow field which is bounded on one side by a solid surface.

3 The actuator disk model

The actuator disk model is a rather well established approximation describing propeller behavior in flow fields to be found in many textbooks, e.g. Prandtl and Tiedjens [8]. In the standard formulation the actuator disk describes a pressure jump across the circular disk with a diameter $D=2R_p$ corresponding to the area covered by the rotating propeller blades.
The actuator disk approximation is compatible with the definitions of the thrust coefficient c_T and the advance ratio J:

$$c_T = \frac{T}{\rho n^2 D^4} \qquad (4)$$

$$J = \frac{V_\infty}{nD} \qquad (5)$$

$$T_c = \frac{T}{\rho V_\infty^2 D^2} = c_T / J^2 \qquad (6)$$

The above definitions are also valid as general descriptions of propulsion performance, without the need to define the actuator disk as a model of propulsion.

The standard actuator disk model assumes a “symmetrical” behavior of the propeller in-and outflow. In the incompressible flow limit, it is assumed that the far fields, both up-and downstream, maintain ambient pressure and half of the thrust is generated by the propeller suction side and half of it on the pressure side.

As a consequence, the contraction ratio of the slipstream is continuous and equal across the actuator disk (propeller) and the minimum slipstream radius R_s is given by $R_s/R_P=1/\sqrt{2}$. In order to maintain mass conservation in this incompressible model, the contraction upstream of the rotor disk is equal to the contraction downstream, constraining the diameter of the stream tube on the intake side.

Improvements to the simple (but useful) model have been manifold. A good overview of different possibilities has been provided by Van Kuik [9], who also provided an improved model by accounting for disk side forces resulting from the vortical flow around the edge of the disk. The modeling proposed by Van Kuik produces flow patterns qualitatively similar to the ones observed in the present experiments, figure 2. Another interesting version suitable for numerical modeling and acoustic predictions has been reported by Verweij [10], where the global parameters are not distributed over the whole disk but only over the specific area covered by the propellers in a digitized form and then rotated with the propeller.

The contraction behavior predicted by the standard actuator disk model is not usually visible in our test conditions. More typical cases are those where the contraction occurs upstream of the propeller, and the slipstream exhibits, apart from the outer domain affected by the blade-tip vortex removing mass out of it, a constant diameter characterized by parallel streamlines, see figure 2. A similar behavior can be observed in many of the snapshots of real aircraft where the condensation occurring in the blade-tip vortex indicates the outer perimeter of the propeller slipstream, and where no discernible contraction of it can be identified, see figure 3 [11] or refer also to the conditions discussed by Roosenboom [13].

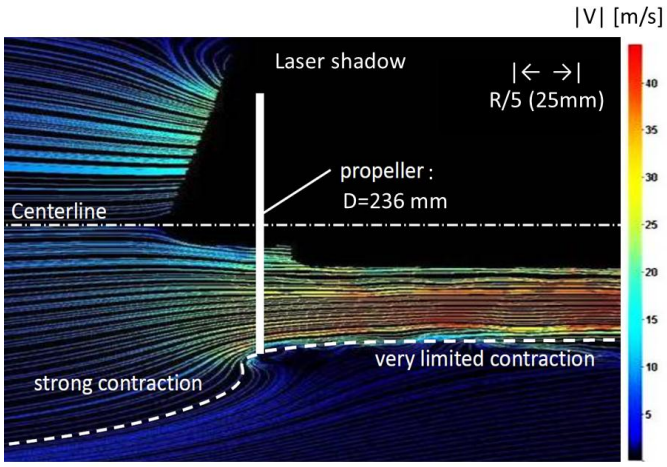

Figure2. Pathlines of velocity magnitude by PIV $C_T \approx 0.37$, $V_\infty=0$ m/s

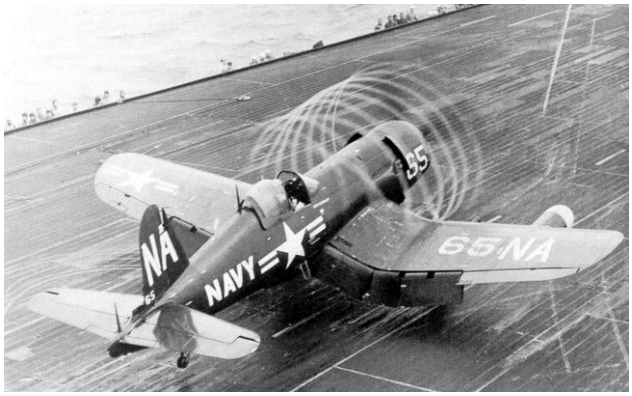

Figure 3. Propeller slipstream condensation of Vought-F4U-Corsair[11].

This behavior is plausible, given that modern propeller blades are designed as airfoils with suction sides providing most of the pressure difference to the free stream; the pressure side contribution is usually maintained very small either using specific designs, Horstman *et al.* [12], or by using standard NACA profiles. A representative calculation of the pressure distribution for a number of NACA profiles at ¼ chord, figure 4, illustrates the characteristic pressure distribution on either side of the airfoils. This illustration supports the observation that the pressure on the downstream side of an actuator disk can be better modeled with setting it equal to the ambient pressure than by distributing the thrust equally between the two sides.

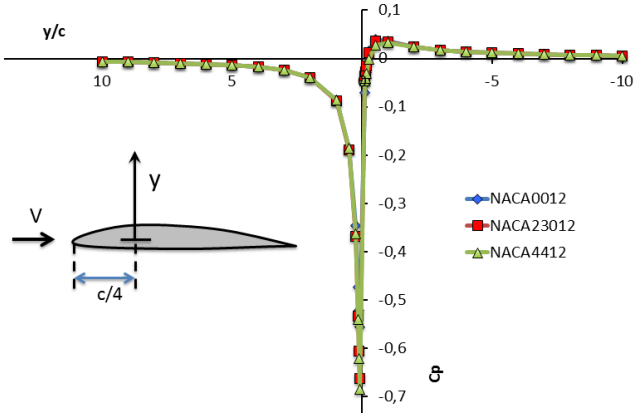

Figure 4. Pressure distributions for four NACA profiles at a constant lift coefficient at quarter chord.

By setting the pressure on the downstream side of the actuator disk p_2 equal to the ambient pressure p_∞, the stream tube contraction ahead of the propeller plane expressed as the ratio of the cross-sectional areas of the upstream stream tube to the propeller disk can be obtained as:

$$\frac{S_\infty}{S_p} = \sqrt{1 + \frac{8}{\pi} T_c} = \sqrt{1 + \frac{8}{\pi} \frac{c_T}{J^2}} \qquad (7)$$

One of the characteristic differences to the standard model here is the possibility of the stream tube to have an infinite contraction ratio when the thrust is maintained at a finite level but the advance ratio is reduced to zero.

As discussed above, one of the requirements for the production of wall-normal vorticity is the presence (or vicinity) of separation resulting in vortex line turning. This is required in addition to a sufficiently high pressure gradient for vorticity flux production in the first place. The presence of separation has also been discussed by some of the authors (e.g. De Siervi *et al.* [1], etc.) as a condition of the occurrence of the ground vortex. The separation clearly must occur, when the intake flow originates on the solid boundary. An estimate of the limiting case of that occurring can be obtained, when the ratio of the stream tube radius far upstream R_∞ is set equal to the height of the propeller disk above ground and compared to the radius of it:

$$\frac{h}{R_p} = \sqrt[4]{1 + \frac{8}{\pi} \frac{k * c_T}{J^2}} = \sqrt[4]{1 + \frac{8}{\pi} k * T_C} \qquad (8)$$

The above relationship can also be expressed, bearing in mind the original definitions of thrust, as relationship between the pressure drop created at the face of the actuator disk (or probably of an engine inlet as well) and the dynamic pressure in the free stream. Thus the limiting streamline case can be expressed by:

$$\frac{h}{R_p} = \sqrt[4]{1 + \frac{2k*(p-p_\infty)}{\rho V_\infty^2}} \qquad (9)$$

In both of the equations above, (8) and (9), an empirical coefficient k has been introduced. Without any interaction with the ground, when the stream tube maintains its axisymmetric shape, $k=1$. In the present study the value of $k=0.55$ is used to account for the stream tube distortion effects; this value is obtained from the experiments and the justification for such a factor can be observed also in figure 2.

Since the pressure drop expressed in equation (9) can be varied independently of the free-stream dynamic pressure, it is not expressed as a pressure coefficient, which the nomenclature would otherwise suggest.

Although the above relationship only describes the stream tube contraction, it is making use of the same pressure relationship which is the driving mechanism for the vorticity generation on the solid surface as well. It does not, however, describe the pressure field outside the actuator disk plain. For describing the pressure distribution outside the limiting stream tube, numerical simulations assuming a steady flow field into and out of the actuator disk were used. In the above approximate evaluation, the flow interaction with the solid surface and deformation of the stream tube as a result of that interaction are considered only in a very global manner. The analysis is mainly used to argue that a linear dependence of the limiting height upon the velocity ratio u_∞/u_i is not the most obvious separation of the domains. Rather, a parabolic (4^{th} order) dependence can be expected to exist. The numerical calculations which were performed can be used to obtain an estimate of the effect of the inflow deformation, which is accounted for by including the

empirical coefficient in the relationship (8) or (9) as discussed above. For the numerical calculations the actuator disk as described in the previous chapter was formulated and implemented in the RANS solver Fluent(TM). The implementation was performed as described in the following paragraph.

4 Numerical model

The mesh of the computational domain was generated by inserting a disk in a semi-cylindrical domain bounded by the far-field conditions and by the ground plane. A pressure-outlet condition is applied on the front area of the actuator disk yielding a pressure drop on the upstream side of the propeller. A velocity-inlet condition is applied on the back area of the disk in order to prescribe both an angular and axial velocity distribution. Symmetry boundary conditions are applied on the semi-cylindrical domain to reduce boundary effects creating interactions with the flow induced by the propeller. Pressure-inlet and pressure-outlet conditions are applied on the inlet and outlet of the domain respectively. The number of mesh nodes is approximately two million; this number is varying according to the height of propeller above the ground. The flow near the propeller is characterized by high streamline curvatures, high pressure gradients, separation and reattachment; this defines the requirement for sufficient grid density in the wall boundary layer. The y^+ value for the boundary layer was set at 10. Non-equilibrium wall condition was used in order to be able to account for the effects of pressure gradient and so on. The so called realizable $k-\epsilon$ model is used, since it was found that the best results for this particular flow field were obtained with this model. This was established in an earlier work by Veldhuis [14] . The number of iterations needed to reach convergence is around ten thousand. Besides, when the continuity and velocity convergence curves become flat and reach the order of 10^{-5} after 7,000 iterations, the net mass flow rate on two sides of the disk is 0.1% of the inflow mass flow rate.

Two versions of the actuator disk model were implemented in the calculation: one without including the slipstream swirl such as described above and one where the slipstream swirl was additionally accounted for. This was done, although the latter presented some complications in regard to the pressure conditions. With the swirl present, the radial acceleration creates an additional pressure drop in the slipstream. At the conditions evaluated, it can be argued that the presence of the swirl does not affect the creation of the ground vortex in a significant manner.

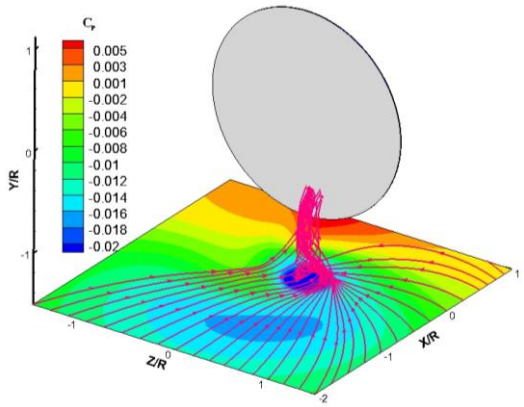

Figure 5. Numerically generated ground vortex. The conditions are: T_c = 51.5,h/r=1.5. Shown is the pressure distribution on the ground as well as the streamlines from half of the upstream domain.

In Figure 5 a representative calculation for one of the experimental cases is presented. The pressure distribution on the ground is represented by the color coded values of the pressure coefficient

$$c_P = \frac{p-p_\infty}{p_\infty - p_1} \qquad (1)$$

where p is the pressure on the ground, p_∞ is the ambient pressure and p_1 is the average pressure on the front disk. In this figure the presence of the vortex is illustrated by plotting the streamlines entering the actuator disk from one half of the upstream domain of the calculations. Since the streamlines from the other half would obscure the view if the vortex core, these were not plotted. Also, the strong circular vortex created at the rim of the actuator disk as a result of the pressure discontinuity in the model (this

corresponds to the presence of a blade tip vortex in real propellers) is excluded from this representation since it does not add to the description of the ground vortex. Thus the single ground vortex originating just underneath the propeller plane is clearly discernible. Performing the same calculation with a symmetrical boundary condition, i.e. reflecting the actuator disk on the ground, will result in a flow field without the vortex entering the actuator disk.

Due to the particular manner of modeling of the actuator disk satisfying the mass conservation requirement but acting as a source term for momentum, the ground vortex does not protrude after the disk, but it terminates in it.

The numerical calculations were performed at a number of conditions in order to verify the domain limitation as described above. The theoretical limit and the corresponding numerically obtained values are plotted in figure 6. The minimum values in this graph are determined by the propeller radius and the propulsion: neither can the propeller be brought closer to a solid surface than the extent of its blade, nor is the thrust reverser case being considered in the present analysis.

Three different states can be identified in the numerical results. These are the state where the vortex clearly enters the actuator disk and the state where there is no roll up of the vortex discernible. A third, in-between state was also obtained in the calculations. This occurred when the the roll-up of a ground vortex was clearly discernible, but it did not enter the actuator disk. This result is identified as a transitional ground vortex in figure 6. The pressure gradient on the ground was sufficient to cause separation, but the suction effect was not sufficient for the vortical flow to reach the propeller plane.

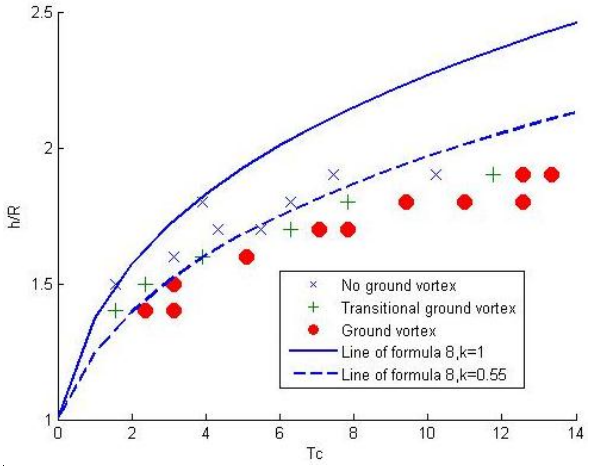

Figure 6. The domain separation for the occurrence or otherwise of the ground vortex.

5 Experimental verification

5.1 Wind-tunnel propeller model and operating regimes

In order to verify the approach described in the previous chapters the numerical calculations have been compared to experimental data obtained by combined oil-flow visualization, measurement of the ground pressure distribution with the help of pressure orifices and PIV measurements. To this purpose a small scale propeller model was installed in the low-speed, closed-circuit wind-tunnel (LTT) of the TU Delft Aerodynamics laboratories. The LTT facility has a cross section of 1.8m width × 1.25 m height and it operates at velocities up to 120 m/s at ambient pressure. The 4-bladed propeller model of 236 mm diameter was installed in the centre of the test section and driven by a 7.5 hp electrical motor, mounted on a supporting sting that provides cooling to the system by means of an internal water circuit. An encoder generating 200 pulses per revolution remotely controlled the frequency of the propeller rotation, maintaining it constant within ±0.3 Hz from the prescribed regime (less than 0.1% at 330 Hz). The propeller was operated at 250 Hz together with a wind-tunnel free-stream velocity of 5~10 m/s. Even when the wind tunnel fan was off, the propeller itself provided enough energy to keep the wind on.

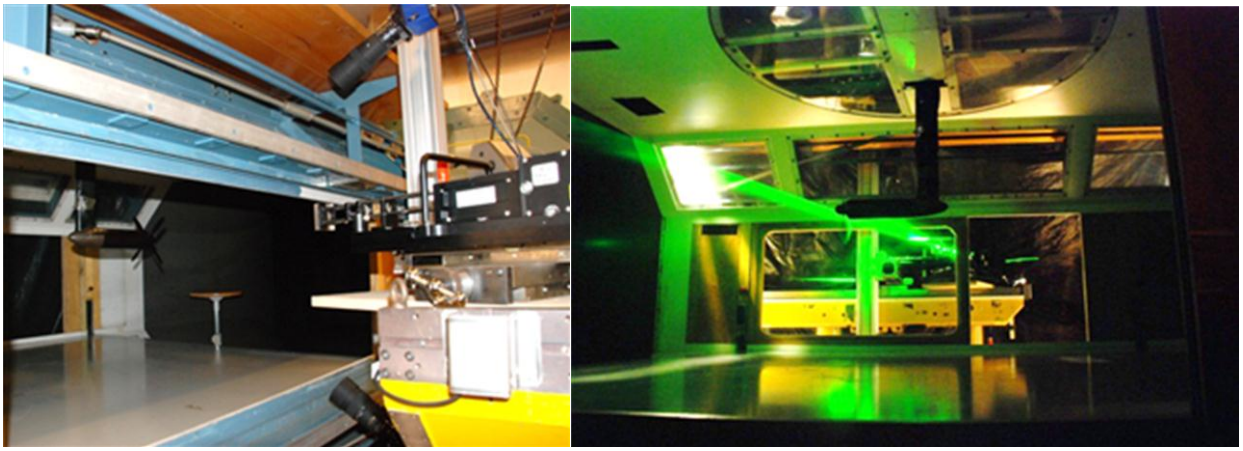

Figure 7. PIV stereoscopic setup and realization

5.2 PIV measurement apparatus

The ground vortex was measured with the help of a stereoscopic PIV arrangement at different heights from the ground. The flow was seeded with particles produced by a SAFEX Twin Fog generator with SAFEX Inside Nebelfluide (mixture of dyethelene-glycol and water, with 1 micron median diameter). The tracer particles were introduced directly downstream of the wind-tunnel test section and uniformly mixed during the recirculation. Laser light was provided by a Quantel CFR200 Nd-Yag laser with 200 mJ/pulse energy, illuminating the field of view through laser optics forming a laser sheet of 2 mm thickness (about 20 cm wide). Two LaVision Imager Pro LX cameras with 4,872×3,248 pixels (10 bit) and two Nikon lenses of 180 mm focal length at $f\#$ 8 were used with the LaVision Davis 7.2 software for acquisition and post-processing. Sets of 140 uncorrelated double-exposure images were recorded at a maximum acquisition frequency of 2.5 Hz. Cameras and laser were simultaneously traversed with the help of a remotely controlled traversing mechanism.

6 Results

For the verification, the wall pressure fields and the velocity fields were extracted from the numerical data. In figure 8 an example of such an extraction is presented, where the velocity field is obtained within the boundary layer at 3 mm from the ground. These velocity vectors can be viewed as representing the wall shear stress pattern on the wall displaying the typical pattern of a focal node leading to separation. Similar data as displayed in figure 9,figure 10 was also obtained in the experiments.

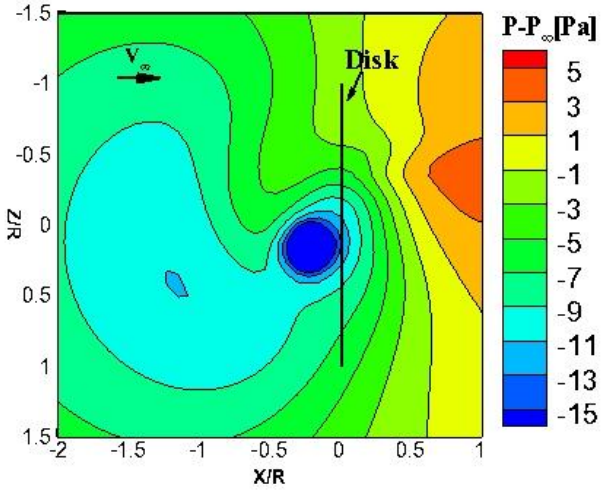

(a)

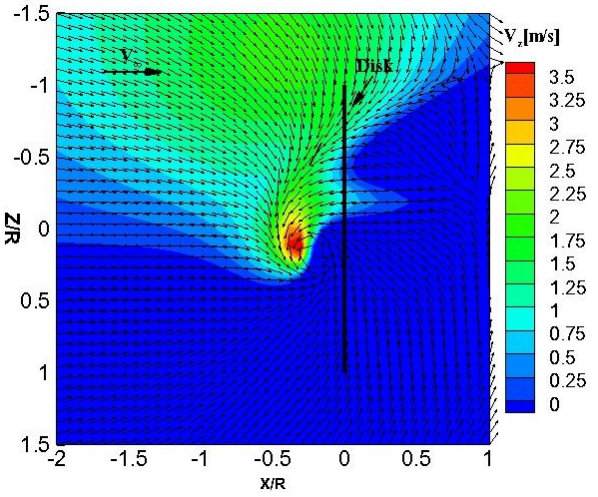

(b)

Figure 8. Simultaneous representation of the ground pressure as well as the velocity field obtained from the numerical calculation:(a) Pressure on the ground plane and (b) velocity obtained at 3 mm from the wall.

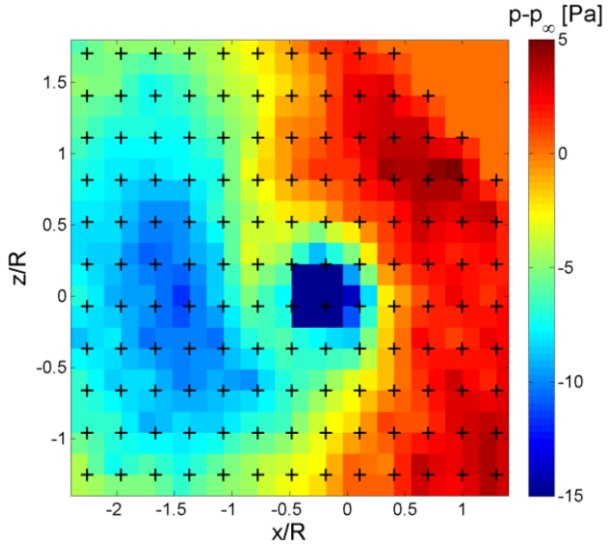

(a)

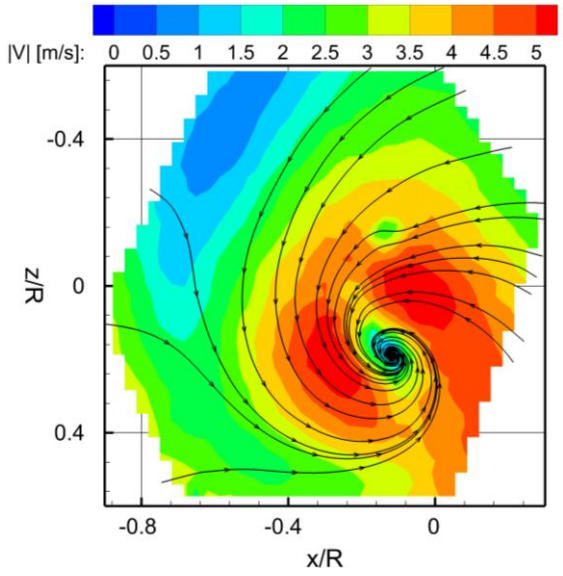

(b)

Figure 9. Experimental results: (a) Pressure on the ground plane, where the crosses denote the locations of the pressure orifices on the ground and (b) velocity from the PIV measurement obtained at 3 mm from the wall in a zoomed in region.

There is general agreement between the averaged results obtained in the wind-tunnel experiments and the steady calculations performed as previously described. The double minimum in the measured pressure field is also reflected in the two areas of vorticity production as visible in figure 5.

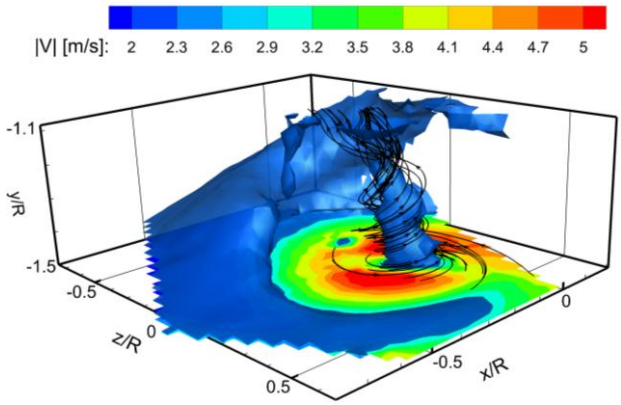

Figure 10. A 3D visualization of velocity magnitude of the ground vortex found in the wind tunnel experiment

In the wind-tunnel experiments some unsteadiness of the flow field was also observed. The significance of this can be estimated with the help of dimensional analysis and is apparently correlated to the product of two non-dimensional parameters, an Euler number *Eu* and a Strouhal number *St*. The unsteadiness is inversely correlated to the ratio of the pressure drop to the dynamic pressure of the free stream, $Eu=(p_\infty-p_1)/(\rho u^2)$, and directly related to the non-dimensional frequency (Strouhal number $St=\upsilon h/u_\infty$) of the propeller induced oscillations of the pressure field. Sufficiently strong suction will tend to stabilize the flow, whereas a large elevation (normalized with the distance of the blade pressure signal convected downstream) above ground will tend to destabilize the vortex.

In our experimental conditions the St was of the order 10 ($St \approx O(10)$), the Euler number was of the same order of magnitude, $Eu \approx O(10)$, although it could go up another order of magnitude in near quiescent flow. The ratio of the two is of order 1, thus at the lower thrust coefficient conditions the propeller induced unsteadiness may affect the comparison of the experiment with the numerical modeling. At higher thrust coefficient conditions, however, the relative significance of the unsteady excitation decreases.

7 Conclusions

The presented results clearly indicate the local nature of the ground vortex. The controlling parameter is the strength of the pressure field (suction) on the ground just under the propeller plane generated by the propulsive action of the propellers relative to the dynamic pressure of the free stream. The experimental evidence so far was obtained only in headwind or quiescent conditions, but there is no indication that adding another velocity component to the free stream flow field will change the conclusions drawn above.

In the wind tunnel experiments there is reported evidence (DNW internal instructions for ground simulation in thrust reverser testing [15]), that the introduction of the motion of the floor, i.e. the removal of the tunnel wall boundary layer by moving the floor at the same speed as the air, does affect the occurrence of the ground vortex. Similar observations were reported by Bosnyakov [16] in a study for a wind tunnel floor whereas Murphy, MacManus and Sheaf [17] studied the strength of the vortex as a function of the wind tunnel boundary layer presence. The removal of the tunnel boundary layer delays the onset of the ground vortex. This observation agrees with the approach developed above, where it is the ratio of the pressure drop in the suction plane compared to the dynamic pressure of the free stream (equation 9) that determines the ground vortex domain boundary. In the presence of a boundary layer, the dynamic pressure is reduced within it, thereby leading to an earlier onset of separation. This observation could also be used in further work for analyzing and controlling the ground vortex mechanism in side wind conditions as well as for the pressure fields in the presence of deployment of thrust reversers. Further refinements to the current study should consider the presence of a wing and the possibilities of manipulating the pressure field by deliberate variations of the suction pressure on the ground, possibly utilizing the thrust reverser flow. Further, the ground roughness height could also affect the separation and thereby the onset of the ground vortex. The unsteady effects might deserve further study as well.

Acknowledgement

The authors acknowledge the participation and the contributions in the experimental campaign of A. Saathoff, currently a lecturer at InHolland.

References

[1] De Siervi F, Viguier H.C., Greitzer E.M., Tan C.S.. Mechanisms of inlet-vortex formation. *J. Fluid Mech.*, Vol. 124, pp 173-207, 1982.

[2] Murphy J.P.. Intake Ground vortex Aerodynamics. PhD. thesis, Cranfield University, 2008.

[3] Murphy J.P., MacManus D.G.. Inlet ground vortex aerodynamics under headwind conditions. *Aerospace Science and Tech.*, Vol. 15, no. 3, pp 207-215, 2010.

[4] Lighthill M.J.. Boundary layer theory. Oxford University Press, Oxford.

[5] Wu J.Z., Wu J.M.. Interactions between a solid surface and a viscous compressible flow field. *J. Fluid Mech.*, Vol. 254, pp 183-211, 1993.

[6] Wu J.Z., Wu J.M.. Vorticity dynamics on boundaries. *Advances in Applied Mech.*, Vol. 32, 1996.

[7] Fric T.F., Roshko A.. Vortical structure in the wake of a transverse jet. *J. Fluid Mech.* Vol. 279, pp 1-47, 1994.

[8] Prandtl L., Tiedjens O.K.G.. Fundamentals of hydro-and aeromechanics. Dover Publications, New York.

[9] Van Kuik G.. On the limitations of Froude's actuator disk concept. PhD. Thesis, University of Twente, 1988.

[10] Verweij A.P.. An investigation in actuator disc CFD solution applicability for aeroacoustic analysis of propellers and rotors. Report TUTwente, 2010.

[11] http://explow.com/Vought_F4U_Corsair.

[12] H. Zimmer, R. Hoffmann and K. H. Horstmann. Investigations of modern general aviation propellers. AGARD, Aerodynamics and Acoustics of propellers, Toronto, Canada, C-P-366, 16, pp 247-248, 1984.

[13] E. Roosenboom. Image based measurement techniques for aircraft propeller flow diagnostics. PhD Thesis, Delft University of Technology, pp 11, 2011

[14] Veldhuis L..Propeller Wing Aerodynamic Interference, PhD. Thesis, Technische Universiteit Delft, pp 229, 2005.

[15] Internal communication. DNW, Noordoostpolder, the Netherlands.

[16] Bosnyakov S.. Digital wind tunnel. Idea and realization. Ewa Workshop, Göttingen 2007 and ASTEC, Moscow 2007.

[17] Murphy J.P., MacManus D.G and Sheaf C.T. Experimental Investigation of Intake Ground Vortices During Takeoff. AIAA JOURNAL Vol. 48, No. 3, March 2010.

Copyright Statement